Full-wave modeling of the time domain reflectometry signal in wetted sandy soils using a random microstructure discretization: Comparison with experiments

Fayçal Rejiba, Florence Sagnard, Cyril Schamper

Full-wave modeling of the time domain reflectometry signal in wetted sandy soils using a random microstructure discretization: Comparison with experiments

F. Rejiba,[1] F. Sagnard,[2] and C. Schamper[1]

Received 23 June 2010; revised 27 April 2011; accepted 9 May 2011; published 8 July 2011.

[1] Time domain reflectometry (TDR) is a proven, nondestructive method for the measurement of the permittivity and electrical conductivity of soils, using electromagnetic (EM) waves. Standard interpretation of TDR data leads to the estimation of the soil's equivalent electromagnetic properties since the wavelengths associated with the source signal are considerably greater than the microstructure of the soil. The aforementioned approximation tends to hide an important issue: the influence of the microstructure and phase configuration in the generation of a polarized electric field, which is complicated because of the presence of numerous length scales. In this paper, the influence of the microstructural distribution of each phase on the TDR signal has been studied. We propose a two-step EM modeling technique at a microscale range (200 μm): first, we define an equivalent grain including a thin shell of free water, and second, we solve Maxwell's equations over the discretized, statistically distributed triphasic porous medium. Modeling of the TDR probe with the soil sample was performed using a three-dimensional finite difference time domain scheme. The effectiveness of this hybrid homogenization approach is tested on unsaturated Nemours sand with narrow granulometric fractions. The comparisons made between numerical and experimental results are promising, despite significant assumptions concerning (1) the TDR probe head and the coaxial cable and (2) the assumed effective medium theory homogenization associated with the electromagnetic processes arising locally between the liquid and solid phases at the grain scale.

Citation: Rejiba, F., F. Sagnard, and C. Schamper (2011), Full-wave modeling of the time domain reflectometry signal in wetted sandy soils using a random microstructure discretization: Comparison with experiments, *Water Resour. Res., 47*, W07512, doi:10.1029/2010WR009688.

1. Introduction

[2] Time domain reflectometry (TDR) is widely used as a nondestructive method for the estimation of the effective dielectric permittivity [e.g., *Topp et al.*, 1980; *Robinson et al.*, 2003] and the electrical conductivity [e.g., *Dalton et al.*, 1984] of a soil. The principle of TDR is based on the analysis of the time domain reflections induced by the impedance changes encountered during the propagation of a short-step voltage signal (rise time less than 200 ps) along the metallic rods of the probe embedded in the soil. The real permittivity is deduced from the travel time of the signal, and the electrical conductivity is estimated from the reflection coefficient when the voltage signal reaches its DC level.

[3] As the equivalent dielectric permittivity is strongly dependent on the soil's microstructure and on the phase configuration, modeling of the TDR transmission line requires a description of (1) the propagation of a guided transverse electromagnetic (TEM) wave along metallic rods connected to a coaxial cable, (2) the TDR probe head, and (3) the soil's microstructure and phase configuration. The best way to take the phase into account is not immediately obvious, as the wavelengths used in TDR measurements are far greater than the microstructure scale of the soil.

[4] TDR interpretation suggests that in the long-wavelength limit, the observed bulk material should be described almost completely by an effective permittivity. The traditional transmission line approach considers a successive series of impedances [*Huebner and Kupfer*, 2007]. In the frequency domain, dielectric spectroscopy is widely used for synthetic materials characterization, as well as for high-speed digital design [e.g., *Tanaka et al.*, 1999], and it is also used in soil science [*Lin*, 2003; *Schaap et al.*, 2003; *Liu*, 2007; *Minet et al.*, 2010]. Both semianalytical and analogical modeling have been used to study homogeneous, frequency-dependant, or one-dimensional materials; however, each of these methods has its own limitations. Several studies dedicated to composite materials have clearly demonstrated that in the mixture the spatial arrangement of the different phases and their potentially strong anisotropy are reflected by the manner in which local fields are established. Such effects have been illustrated using finite difference [*Karkkainen et al.*, 2000, 2001] or finite

[1]UMR Sisyphe, Université Pierre et Marie Curie–Paris 6, Paris, France.
[2]Laboratoire Central des Ponts et Chaussées, MACS, Paris, France.

0043-1397/11/2010WR009688

element methods [*Myroshnychenko and Brosseau*, 2005; *Wang and Pan*, 2007; *Bolvin and Chambarel*, 2007]. In addition, there is a serious issue with the inverse problem, which is ill conditioned since many microstructural configurations could produce the same effective permittivity, and because of the excessive sensitivity of the TDR signal associated with the permittivity of any of the phases. These observations, which have been crucial in homogenization problems (condensed matter, porous media, and the vadose zone), suggest that the relationship between the microstructural configuration and the effective permittivity is not trivial, not only because of the multitude of length scales but also because it is difficult to perform accurate experimental validations.

[5] The work presented in the present paper is an extension of developments made by *Rejiba et al.* [2005], which were focused on sensitivity analysis of a synthetic TDR signal. We propose full-wave modeling in three dimensions (3-D) based on the finite difference time domain (FDTD) approach, with specific numerical developments related to the coaxial cable and the TDR probe head. Moreover, we provide a statistical description of the three phases of the soil made for an unsaturated, clay-free sand.

[6] The TDR device, made with a two-rod metallic waveguide that is 8 cm in length with a rod separation of 1.2 cm, was connected to a coaxial cable with a characteristic impedance of 50 Ω. The section of each rod is 4 mm^2, and the probe head is made of a parallelepiped 1 cm × 1 cm × 2 cm epoxy resin body. Usually, the coaxial cable modeling over a 3-D FDTD grid is achieved using a "thin-wire" formalism in order to solve for the currents and voltages in one dimension, which allows the six components of the electromagnetic field to be determined using the circulation and flux relations on the basis of Ampère's and Faraday's laws [*Maloney et al.*, 1994; *Hockanson et al.*, 1996]. As the accurate electromagnetic characteristics of the TDR probe head are rarely available, we evaluated equivalent permittivity values for both the coaxial cable and the TDR probe head.

[7] An important step in the current soil modeling approach relies on the definition of a dielectric, geometrical three-phase model for the soil, which provides a reasonable compromise between a homogeneous model and the real porous model with all its phases. The electrical conductivity associated with the present discretization is nonzero only for the water phase, which in this case corresponds to tap water.

[8] The spatial sampling was set to match the centroid grain size of 200 μm of a Nemours sand characterized by a narrow granulometric fraction, thus defining the minimal modeled pore volume. However, this discretization appears to be too coarse to accurately describe the pore and water distributions. In order to improve the given coarse three-phase model without refining the discretization (which would quickly lead to an overburden of computational resources), it was decided to define an equivalent grain permittivity for the solid fraction. The equivalent grain was represented by a coated sphere, with a thin shell of free water. The equivalent "grain" permittivity defined for each FDTD grain cell was estimated using the effective medium theory (EMT) [*Torquato*, 2002; *Cosenza et al.*, 2009].

[9] The equivalent permittivities associated with the coaxial cable and the probe head were estimated in order to fit experimental reflection coefficients. A calibration was made using NaCl solutions at several concentrations, with conductivities ranging from 2 to 210 μS/m, and also with tap water (581 μS/m), air, and a probe head short circuit in order to match the amplitude level of the first reflection coefficient. It should be noted that although this calibration step leads to a correct estimation of the mean level of reflection, it does not permit accurate modeling of all local discrepancies occurring at the beginning of the reflected signal.

[10] Modeling of the TDR probe embedded in a heterogeneous soil was compared with measurements associated with several sand samples (Nemours sand) characterized by different water contents. The results of these comparisons provided an opportunity to evaluate and discuss the relevance of a mixed discretization-homgenization approach for the characterization of triphasic porous media measured by a TDR probe.

2. Modeling of the TDR Transmission Line

[11] Under the source-free assumption, for an isotropic and heterogeneous distribution of dielectric permittivity and electrical conductivity, the transient electromagnetic field is described by the following time domain Maxwell's equations:

$$\begin{aligned} \frac{\partial \tilde{D}}{\partial t} &= \frac{1}{\sqrt{\epsilon_0 \mu_0}} \nabla \times H, \\ \tilde{D}(\omega) &= \epsilon_r^*(\omega) \tilde{E}(\omega), \\ \frac{\partial H}{\partial t} &= -\frac{1}{\sqrt{\epsilon_0 \mu_0}} \nabla \times E, \end{aligned} \tag{1}$$

where H is the magnetic field, ω is the angular frequency, and ϵ_0 and μ_0 are the free space dielectric permittivity and magnetic permeability, respectively. $\tilde{E}$ and $\tilde{D}$ are the normalized electric field and the normalized electric flux density, respectively:

$$\begin{aligned} \tilde{E} &= \sqrt{\frac{\epsilon_0}{\mu_0}} E, \\ \tilde{D} &= \sqrt{\frac{1}{\epsilon_0 \mu_0}} D. \end{aligned} \tag{2}$$

[12] In the present study, the effective soil permittivity model $\epsilon_r^*(\omega, x, y, z)$ includes a real relative permittivity $\epsilon(x, y, z)$ and a conductivity $\sigma(x, y, z)$ at each FDTD cell location, leading to the following relationship:

$$\epsilon_r^*(\omega, x, y, z) = \epsilon(x, y, z) + \frac{\sigma(x, y, z)}{j\omega\epsilon_0}, \tag{3}$$

where $j^2 = -1$.

[13] The 3-D FDTD computation of Maxwell's equations was made according to Yee's standard staggered algorithm [*Yee*, 1966], which is second order accurate in time and space. The ramp source, calibrated by means of the air measurement, has a tangential hyperbolic shape and a rise time of 200 ps, leading to frequency domain information

lying below a maximum frequency of 2 GHz. The isotropic spatial step value, equal to 200 μm, is 80 times smaller than the minimum wavelength in water, which is sufficient to avoid significant numerical dispersion. The FDTD–auxiliary differential equation–simplified unsplit perfect matched layer (FDTD-ADE-SUPML) numerical scheme associated with equation (1) has been fully described in the literature [e.g., *Taflove and Hagness*, 2005; *Rejiba et al.*, 2003; *Sullivan*, 2002]. A message-passing interface parallelized version was implemented to allow upscaling and in order to consider finer levels of discretization, which usually lead to significant memory requirements. The routine was executed on the Enabling Grids for E-sciencE (EGEE) distributed memory grid, which is the European cloud computing network.

[14] The two-rod TDR probe and the three-phase porous medium were discretized in an isotropic three-dimensional FDTD grid with perfect matched layer (PML)-like absorbing boundary conditions [*Berenger*, 1994] in order to simulate an open domain; in our case, the anisotropic PML layers, in addition to the simulation domain, required a mesh containing nearly 10 million cells. In practice, the grid has a dimension of 100 × 100 × 1200 cells, including the absorbing conditions. Sufficient space was defined above the air-soil interface to allow the incident voltage $V_0(t)$ to reach its DC level before reaching the air-soil interface.

[15] The TDR probe (Figure 1) is assumed to be excited by a TEM wave that can be modeled either by the presence of a coaxial cable, using the thin-wire formalism, or by a quasi-plane wave using Huygens' principle of superposition (the adopted solution), generated along a line of cells inside the simulation domain border.

[16] In the present study, the coaxial cable is modeled by extending the two rods above the air-soil interface and embedding them into an equivalent medium characterized by a constant real dielectric permittivity ϵ_{eq}. As all impedance contrasts at the probe head location are not fully described, the probe head was modeled by an additional element of constant permittivity ϵ_{hp}. Indeed, as the probe head produces a small bump, observed in previous experiments, it was adjusted experimentally to fit the air and short circuit experiments. In reality, each element of the transmission line contributes to the global losses and is characterized by a frequency-dependent impedance. For reasons of simplicity and because the cable has a length of only 1 m, the corresponding dispersion losses were not modeled.

[17] The equivalent transmission line representing the coaxial cable (a pair of symmetrical, cylindrical twin-wire lines) without its head probe has a characteristic impedance Z_0 expressed as follows [*Ball*, 2002]:

$$Z_0 = \frac{1}{2\pi}\sqrt{\frac{\mu_0}{\epsilon_{eq}\epsilon_0}}\ln\left(F + \sqrt{F^2 - 1}\right), \tag{4}$$

where $F = (S^2 - 2R^2)/2R^2$, S is the separation (center to center) between both rods, and R is the radius of the rod. The FDTD square section of the rods is 4 mm^2, and an equivalent radius R was defined in order to evaluate Z_0.

[18] The excitation defined in the 3-D grid, using a segment source between two perfectly conductive rods, is not a perfect TEM mode as in the case of a coaxial cable because of the naturally occurring spherical 3-D divergent attenuation inherent in Maxwell's equations. In order to force the TEM propagation to take place in the equivalent source medium (in addition to the perfect electrical surface conditions defined at the surface of the metallic rods), the spatial derivation in radial directions must be cancelled in order to approximate the propagation of a plane wave.

[19] Concerning feeding the grid, the electric field excitation E_x (x polarization) is defined on a segment between the rods and has the shape of a ramp function. Such an excitation, known as hard sourcing in the FDTD formalism, acts like a reflector and could interact with the reflected signal, in particular when it reaches its DC value. In order to avoid the occurrence of artificial reflections at the segment location, during simulations made over long periods, the E_x segment source (associated with the source voltage $V_0(t)$) is fed using an equivalent transparent source formulation.

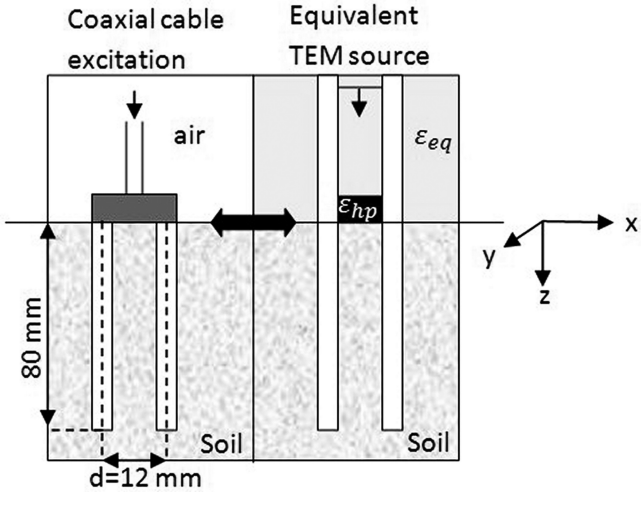

Figure 1. Equivalent time domain reflectometry (TDR) modeling used in the finite difference time domain (FDTD) simulations. The initial feeding model (coaxial cable and head probe) in the air is replaced by an extended two-rod waveguide embedded in equivalent media of permittivity ϵ_{eq} and ϵ_{hp}.

This excitation is perfectly equivalent to the use of a classical current density source, allowing the use of any model associated with optically guided wave measurements. The FDTD grid is thus excited by the equivalent tangential magnetic current source M_y (y polarization), which appears in the magnetic field H_y component [*Wang and Teixeira*, 2003]. The probe voltage $V(t)$ is recorded just below the source location (at a grid step) and is computed from the numerical integration of the electric field E_x situated between the rods (distance $d = 12$ mm). The reflection coefficient $\rho(t)$, which is recorded during a TDR experiment, is finally calculated from both the measured $V(t)$ and the incident $V_0(t)$ time domain voltages as follows:

$$\rho(t) = \frac{V(t) - V_0(t)}{V_0(t)}. \tag{5}$$

3. Microstructural Equivalent Soil Model

[20] In the case described here, the minimum volume corresponding to the cell size (8×10^{-3} mm^3) is too coarse to accurately describe the soil pore-scale structure. The results of our initial simulations on saturated sand have shown few, but nevertheless measurable, differences. The variation in the first level of reflection coefficient is greater than 10%, and the inflection point is situated around half a nanosecond earlier or later when compared to experiments in which the permittivity of the grain (quartz) is maintained at its assumed value of 5.5. The lower and upper limits of simulations in the saturated case correspond to grain permittivities of 5.5 and 8.5, respectively (see Figure 4). This suggests that despite the currently used coarse grid, it is possible to maintain a three-phase description of the medium by means of a local homogenization process.

[21] When dealing with very fine variations in physical properties, the main issue in FDTD modeling consists of using physically and geometrically acceptable homogenization of some of the existing phases over a coarse mesh. Without loss of generality, since a dispersive law is systematically associated with a particular distribution of constant properties, we propose to focus on a single element, which will include all of the physics missing in the initial discretization. This model, like any other model (multilayered, entirely homogeneous, or homogeneous by parts), is closely related to the inverse problem associated with the interpretation of the TDR signal; here we have considered our sample to be a random three-phase distribution, with a discretization corresponding to the centroid size of the grain obtained from the granulometric curve. The homogenization process was applied only to the solid components in order for the grain to be represented by an equivalent dielectric value. Instead of refining the grid size, which would have rapidly overwhelmed memory resources, we defined an equivalent grain permittivity ϵ_{cs} for the case of wet sand. The volumetric electrical conductivity was set to be nonzero only for the water filling.

[22] The permittivity of the solid grain ϵ_s is equal to 5.5, which corresponds to the permittivity of quartz. Nemours sand is a clay-free sand, with a grain size fraction of 90% for the range between 170 and 210 μm and an experimentally estimated porosity ϕ of 40%. The permittivity of the solid grain was adjusted to represent the addition of a thin shell of free water (with a microscale discretization, the distinction between free and bound water is not justified). As shown in Figure 2, a simple, coated sphere model, whose volume is identical to the cubic FDTD cell, allowed us to define an equivalent relative permittivity value for the solid grain. Assuming the thickness of this thin shell of free water ($\epsilon_{water} = 79$ at 20°C) to correspond to nearly 1% of the radius of the equivalent sphere, we obtained a thickness of 1.2 μm; the outer (a) and inner (b) radii of the shell were defined as 120 and 118.8 μm, respectively. Finally, the equivalent permittivity ϵ_{cs} of the cubic FDTD cell was evaluated to be 7, using the EMT mixing law for a coated sphere as follows:

$$\epsilon_{cs} = \epsilon_w \frac{\epsilon_s + 2\epsilon_w + 2f(\epsilon_s - \epsilon_w)}{\epsilon_s + 2\epsilon_w - f(\epsilon_s - \epsilon_w)}, \tag{6}$$

where $f = (a/b)^3$ represents the filling factor.

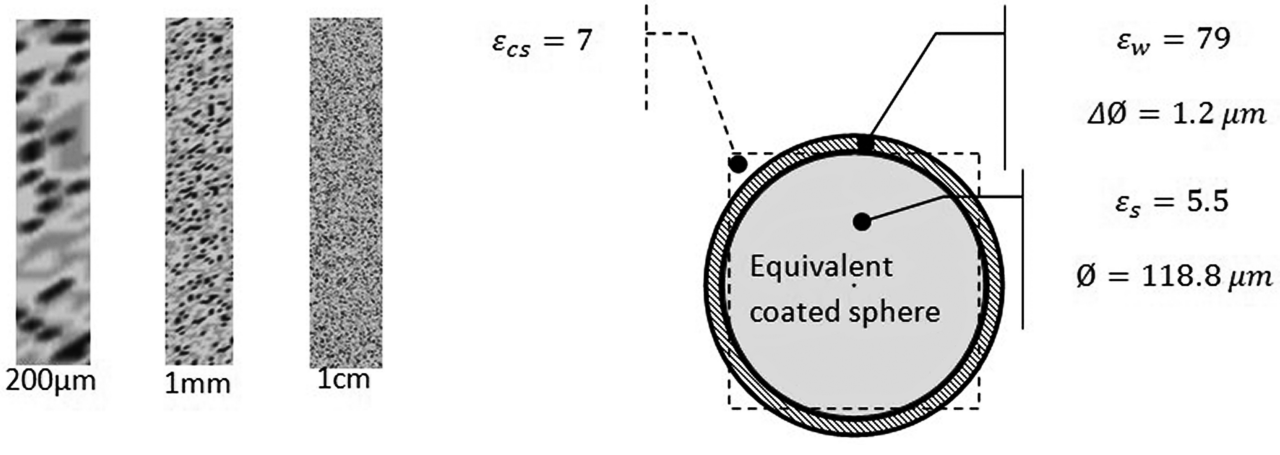

Figure 2. Equivalent medium theory applied to a coated sphere. (left) View of the modeled microstructure at several different scales: air (dark gray) and water (light gray) distributions. (right) Equivalent water-coated sphere model (cross-sectional view) used to approximate the permittivity of the grain (ϵ_{cs}) in a cubic FDTD cell, using an effective medium theory mixing law.

[23] The microstructure and phase configuration of the soil, corresponding to the porosity and water fractions, respectively, were then distributed over the FDTD grid using a discrete binomial distribution (Figure 2) in the following manner: first, the solid and the pores were associated with a success probability $p_1 = 1 - \theta$ (i.e., of the cell being filled with a solid); second, the cells that had previously been considered to be pores were set according to another binomial distribution, but with a success probability $p_2 = \theta/\phi$ (i.e., of the cell being filled with water) corresponding to the degree of saturation. The discrete binomial distribution has a probability density function that can be expressed as follows:

$$f(k|n,p) = \binom{n}{k} p^k (1-p)^{n-k} \quad k = 0, 1, 2, ..., n, \tag{7}$$

where k is the number of successes in n trials of a Bernoulli process, having a success probability equal to p.

4. Calibration of the Transmission Line Model

[24] The soil measurements were made using a TDR100 system (Campbell Scientific). Following calibration of the excitation signal, using the air and short circuit measurements, the equivalent permittivities ϵ_{eq} and ϵ_{hp} (see Figure 1) were fitted by minimizing the root-mean-square errors between the first level of reflection obtained for several NaCl solutions and the FDTD simulations. The optimal values of ϵ_{eq} and ϵ_{hp} were estimated to be 12.8 and 31.2, respectively. It should be noted that the former equivalent permittivities include the characteristic impedance as well as the FDTD intrinsic lattice impedance. In addition, they should not be compared with the permittivities of the corresponding material, but rather with the corresponding impedance contrast.

[25] From Figure 3, it can be seen that the modeled TDR signals differ slightly from the experimental results (~5% errors). This outcome is probably due to the presence of a nonperfect TEM source excitation, to numerical dispersion, and to physical dispersion (currently not modeled) associated with the head probe.

5. Numerical Versus Experimental Results

[26] Figure 4 shows several experimental TDR traces and their corresponding numerical models in sand samples, as well as air and head probe short-circuited measurements. Despite local mismatches for the first amplitude bumping, the modeled and experimental signals are similar. Concerning the three samples with different water contents (12%, 27%, and saturated at 40%), we also observe similar overall trends.

[27] Nonuniform discrepancies (for the different water contents) at the beginning of the signal are more likely because of two main effects: (1) the differences in the immediate proximity of random media generation can lead to significant local dielectric anomalies and (2) the hand-mixed samples, particularly in the unsaturated case, are not completely homogeneous, particularly at their free surfaces. To a lesser extent, the numerical assumptions associated with the TEM source initialization, e.g., the coarse discretization, and the absence of frequency-dependent

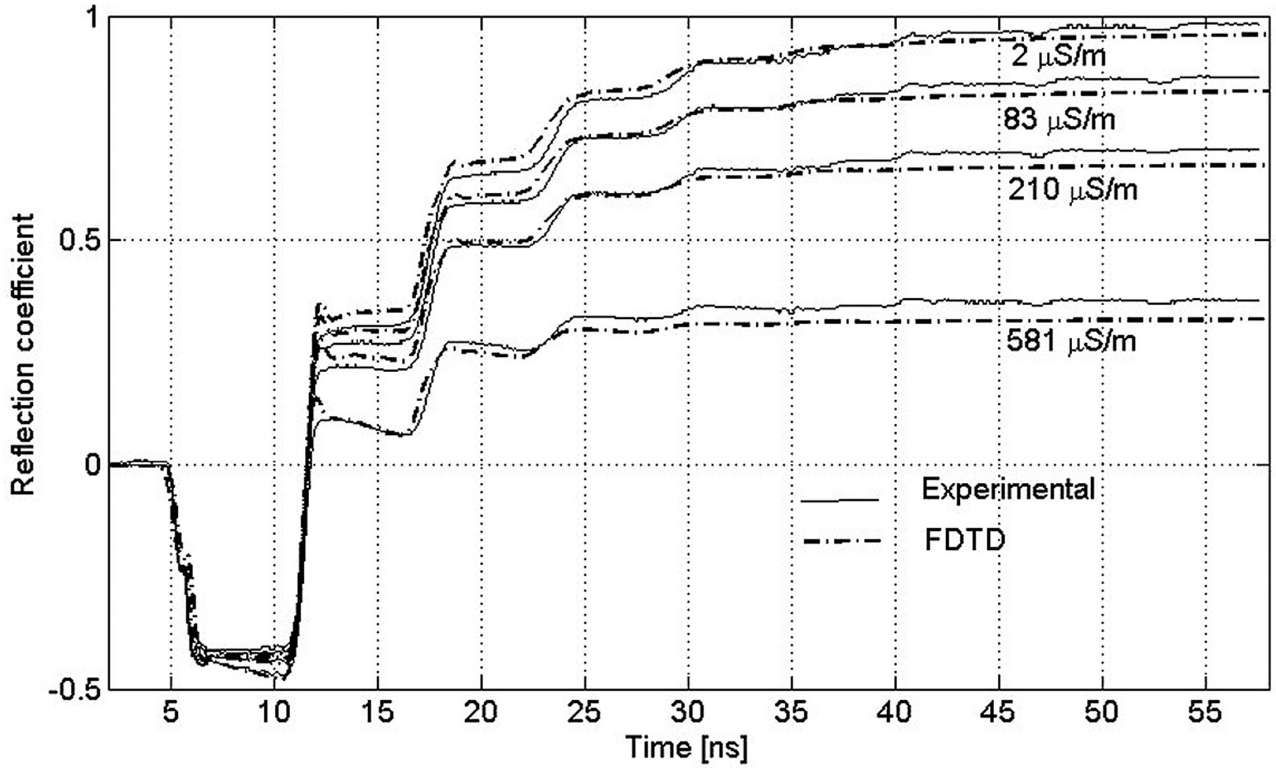

Figure 3. Experimental and theoretical TDR reflection coefficients obtained on several NaCl solutions and used for the evaluation of the equivalent permittivities ϵ_{eq} and ϵ_{hp} (see Figure 1).

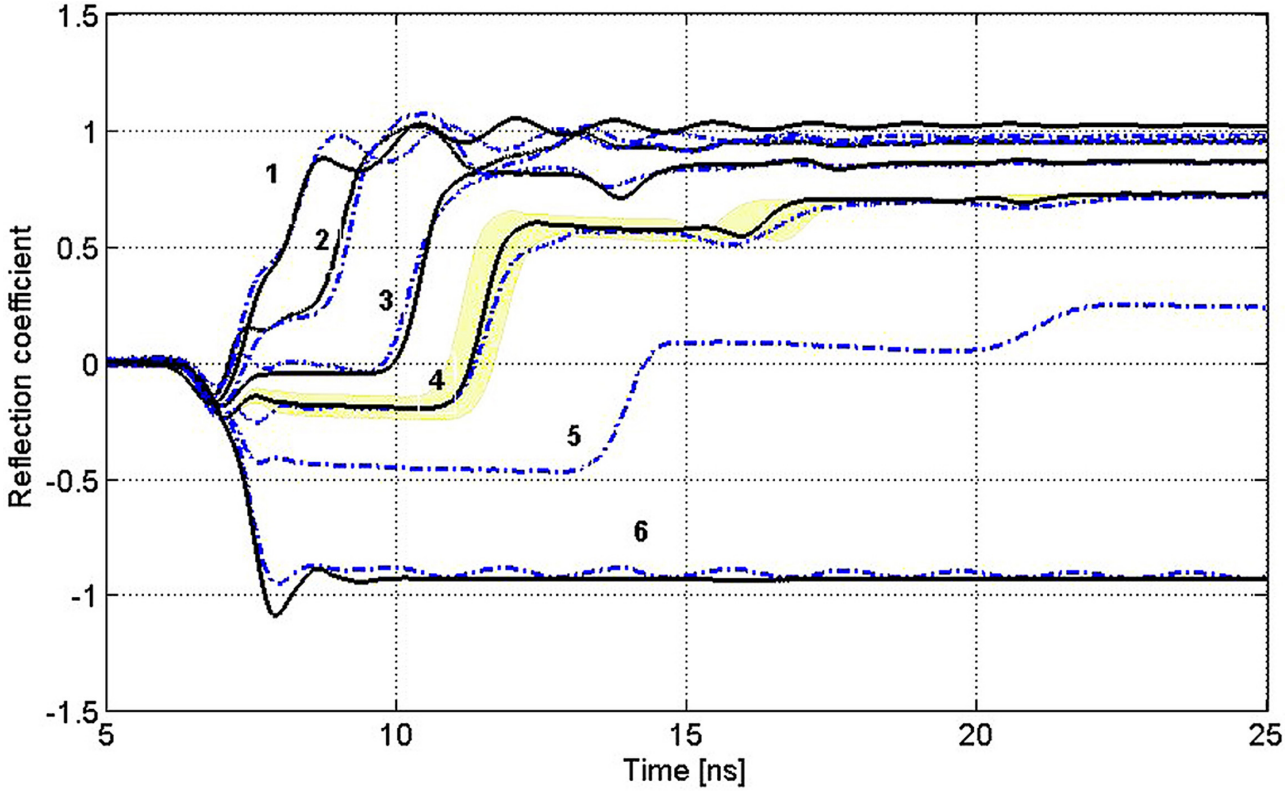

Figure 4. Comparison of experimental (dashed line) and FDTD simulations ($\Delta x = \Delta y = \Delta z = 200$ μm) for the cases of 1, air; 2, $\theta = 12\%$; 3, $\theta = 27\%$; 4, saturation ($\theta = 40\%$). Line 6 shows a short circuit at the head probe location. Line 5 represents the measurements made with the tap water used in the experiment ($\sigma = 581$ μS/m). The lower and upper limits of the shaded area correspond to simulations in the saturated case, associated with grain permittivities of 5.5 and 8.5, respectively. This shows that the best fit with the experimental data is found for a grain permittivity equal to 7.

impedances associated with the equivalent head probe and source domain are all potential sources of amplitude errors.

6. Discussion and Conclusions

[28] In this paper, the FDTD modeling of the TDR probe and the sample consists of several steps:

[29] 1. The equivalent and constant permittivity for the equivalent TEM wave source corresponding to the coaxial cable (ϵ_{eq}) and the equivalent head probe permittivity (ϵ_{hp}) were fitted to match a representative range of known samples.

[30] 2. The sand microstructure was coarsely discretized at the micrometer scale, according to the centroid size of an equivalent grain (200 μm).

[31] 3. The equivalent permittivity of a grain, representing a simple coated solid sphere surrounded by a thin shell of free water, was evaluated using the equivalent medium theory.

[32] 4. The TEM excitation was defined by an equivalent and transparent magnetic source. The shape of the source was calibrated using the air measurement.

[33] These conceptual and numerical assumptions lead to two main types of error: (1) local errors associated with close time bumping and (2) DC level drifts after long time intervals.

[34] The first type of error is more likely to occur because of the probe head definition, uncertainties concerning the real and modeled three-phase random distribution at the air sample surface, and nonuniformities in the contact between the probe head and the soil. The second type of error results from imperfect TEM excitation, the frequency-independent equivalent permittivities defined for the coaxial cable and the probe head, and the poor estimation of the real pore connectivity and surface conductivity inherent in the coarse mesh. The source function with a hyperbolic tangent shape is calibrated using the TDR air measurement but is also associated with inevitable data fitting errors.

[35] The specific choice of FDTD grid excitation with an equivalent magnetic moment, instead of a classical current density, appears to be a particularly elegant approach since it could also be used for possible fiber-optic devices, which are usually designed for dielectric or temperature measurements.

[36] The present triphasic and microstructural medium description is certainly too coarse to quantify all the various polarization processes. As the sample was arranged with no particular precaution, a binomial distribution for each phase, associated with its respective proportion, was used as a trade-off between the conflicting needs of model representativity and computational resource requirements (the current

simulations for a single TDR trace, using a recent eight-node cluster, take approximately 2 h). In a first modeling step, it was useful to consider a mixed homogenization approach, which in our case was focused on a coated sphere grain model. This approach offers a high degree of flexibility and has produced satisfactory results with almost homogeneous sand. Moreover, it allows the modeler to test any phase-mixing arrangement for the purposes of sensitivity studies using any available 3-D FDTD free code, such as that provided by the MEEP project [*Oskooi et al.*, 2010].

[37] The main difficulty with this approach lies in the experimental validation, which is strongly dependent on the knowledge of the sample used for the experiment. In the present case, the use of wet sand with narrow granulometric fractions limits the degree to which the representative soil models can make the sample suitable for the validation exercise. Clay-sand mixtures could be the next target to be used for the purposes of validation, but they would at least require multidimensional scanning electron microscopy, followed by mathematical morphology analysis, in order to correctly estimate the statistical parameters associated with each phase; even under these conditions, it will inevitably be necessary to coarsen the mesh and define local equivalent properties.

[38] The modeling methodology presented and applied in this paper shows that a 3-D full-wave finite difference time domain approach, associated with fine isotropic gridding, makes it possible to analyze the influence of a given multiphase configuration, presently at the microscale, on TDR measurements. As described in section 1, conventional partial differential equation (PDE) solvers (FDTD and FEM) were used to solve the classical electric potential transport equation for porous media in two dimensions and for a two-phase mixture in order to estimate an equivalent permittivity. To the best of our knowledge, the TDR sensor itself had never previously been associated with three-dimensional full-wave studies dedicated to soil sciences. Such modeling requires (1) significant grid refinement for complex structures and, above all, (2) an accurate description of the electromagnetic phenomena arising at the interfaces between all phases. It is not currently possible to achieve the latter requirement using discretization associated with PDE solvers. The second point, which is addressed in this study through the use of EMT applied to the grain-water pair, is still unsatisfactory from the point of view of a physical understanding. These interface constraints, associated with potential and flux continuities in a porous medium, have recently been studied using methods based on stochastic-statistical theories, such as the lattice gas automata or the lattice Boltzmann method, to predict the electric transport properties in two-dimensional multiphase porous media [e.g., *Wang and Pan*, 2007, 2008; *De*, 2008]. This is probably one of the most promising directions for progress in full-wave TDR modeling of porous media.

[39] **Acknowledgments.** This study makes use of results produced by the Enabling Grids for E-sciencE project, a project cofounded by the European Commission (under contract number INFSO-RI-031688) through the Sixth Framework Programme (FP6). The authors would also like to thank the Calculation and Research Centre (CCR) of the Pierre and Marie Curie University (Paris, France) for providing access to its JS21 and JS22IBM machines. Finally, we would like to thank two anonymous reviewers, who have provided thoughtful comments that significantly improved the quality of this study.

References

Ball, J. (2002), Characteristic impedance of unbalanced TDR probes, *IEEE Trans. Instrum. Meas.*, *51*(3), 532–536.

Berenger, J. (1994), A perfectly matched layer for the absorption of electromagnetic waves, *J. Comput. Phys.*, *114*(2), 185–200.

Bolvin, H., and A. Chambarel (2007), Electromagnetic wave propagation in polarizable wet media: Application to a TDR probe, *Meas. Sci. Technol.*, *18*(4), 1105–1109.

Cosenza, P., A. Ghorbani, C. Camerlynck, F. Rejiba, R. Guérin, and A. Tabbagh (2009), Effective medium theories for modelling the relationships between electromagnetic properties and hydrological variables in geomaterials: A review, *Near Surf. Geophys*, *7*, 563–578.

Dalton, F., W. Herkelrath, D. Rawlins, and J. Rhoades (1984), Time-domain reflectometry: Simultaneous measurement of soil water content and electrical conductivity with a single probe, *Science*, *224*(4652), 989–990, doi:10.1126/science.224.4652.989.

De, A. (2008), Numerical modeling of microscale mixing using lattice Boltzmann method, Ph.D. thesis, Va. Polytech. Inst. and State Univ., Blacksburg.

Hockanson, D., J. Drewniak, T. Hubing, and T. Van Doren (1996), FDTD modeling of common-mode radiation from cables, *IEEE Trans. Electromagn. Compat.*, *38*(3), 376–387.

Huebner, C., and K. Kupfer (2007), Modelling of electromagnetic wave propagation along transmission lines in inhomogeneous media, *Meas. Sci. Technol.*, *18*(4), 1147–1154.

Karkkainen, K., A. Sihvola, and K. Nikoskinen (2000), Effective permittivity of mixtures: Numerical validation by the FDTD method, *IEEE Trans. Geosci. Remote Sens.*, *38*(3), 1303–1308.

Karkkainen, K., A. Sihvola, and K. Nikoskinen (2001), Analysis of a three-dimensional dielectric mixture with finite difference method, *IEEE Trans. Geosci. Remote Sens.*, *39*(5), 1013–1018.

Lin, C. (2003), Frequency domain versus travel time analyses of TDR waveforms for soil moisture measurements, *Soil Sci. Soc. Am. J.*, *67*(3), 720–729.

Liu, N. (2007), Soil and site characterization using electromagnetic waves, Ph.D. thesis, Va. Polytech. Inst. and State Univ., Blacksburg, Va.

Maloney, J., K. Shlager, and G. Smith (1994), A simple FDTD model for transient excitation of antennas by transmission lines, *IEEE Trans. Antennas Propag.*, *42*(2), 289–292.

Minet, J., S. Lambot, G. Delaide, J. Huisman, H. Vereecken, and M. Vanclooster (2010), A generalized frequency domain reflectometry modeling technique for soil electrical properties determination, *Vadose Zone J.*, *9*(4), 1063–1072.

Myroshnychenko, V., and C. Brosseau (2005), Finite-element method for calculation of the effective permittivity of random inhomogeneous media, *Phys. Rev. E*, *71*(1), 016701.

Oskooi, A. F., D. Roundy, M. Ibanescu, P. Bermel, J. D. Joannopoulos, and S. G. Johnson (2010), MEEP: A flexible free-software package for electromagnetic simulations by the FDTD method, *Comput. Phys. Commun.*, *181*, 687–702, doi:10.1016/j.cpc.2009.11.008.

Rejiba, F., C. Camerlynck, and P. Mechler (2003), FDTD-SUPML-ADE simulation for ground-penetrating radar modeling, *Radio Sci.*, *38*(1), 1005, doi:10.1029/2001RS002595.

Rejiba, F., P. Cosenza, C. Camerlynck, and A. Tabbagh (2005), Three-dimensional transient electromagnetic modeling for investigating the spatial sensitivity of time domain reflectometry measurements, *Water Resour. Res.*, *41*, W09411, doi:10.1029/2004WR003505.

Robinson, D., S. Jones, J. Wraith, D. Or, and S. Friedman (2003), A review of advances in dielectric and electrical conductivity measurement in soils using time domain reflectometry, *Vadose Zone J.*, *2*(4), 444–475.

Schaap, M., D. Robinson, S. Friedman, and A. Lazar (2003), Measurement and modeling of the TDR signal propagation through layered dielectric media, *Soil Sci. Soc. Am. J.*, *67*(4), 1113–1121.

Sullivan, D. (2002), An unsplit step 3-D PML for use with the FDTD method, *IEEE Microwave Guided Wave Lett.*, *7*(7), 184–186.

Taflove, A., and S. Hagness (2005), *Computational Electrodynamics: The Finite-Difference Time Domain Method*, 3rd ed., Artech House, Boston.

Tanaka, M., W. Cui, X. Luo, J. L. Drewniak, T. H. Hubing, T. P. van Doren, and R. E. DuBroff (1999), FDTD modeling of EMI antennas, in *1999 International Symposium on Electromagnetic Compatibility*, pp. 560–563, IEEE, New York, doi:10.1109/ELMAGC.1999.801389.

Topp, G., J. Davis, and A. Annan (1980), Electromagnetic determination of soil water content: Measurements in coaxial transmission lines, *Water Resour. Res.*, *16*(3), 574–582, doi:10.1029/WR016i003p00574.

Torquato, S. (2002), *Random Heterogeneous Materials: Microstructure and Macroscopic Properties*, Springer, New York.

Wang, M., and N. Pan (2007), Numerical analyses of effective dielectric constant of multiphase microporous media, *J. Appl. Phys.*, *101*, 114102.

Wang, M., and N. Pan (2008), Predictions of effective physical properties of complex multiphase materials, *Mater. Sci. Eng. R*, *63*(1), 1–30.

Wang, S., and F. Teixeira (2003), An equivalent electric field source for wideband FDTD simulations of waveguide discontinuities, *IEEE Microwave Wireless Compon. Lett.*, *13*(1), 27–29, doi:10.1109/LMWC.2002.807714.

Yee, K. (1966), Numerical solution of initial boundary value problems involving Maxwell's equations in isotropic media, *IEEE Trans. Antennas Propag.*, *14*(3), 302–307, doi:10.1109/TAP.1966.1138693.

F. Rejiba and C. Schamper, UMR Sisyphe, Université Pierre et Marie Curie–Paris 6, Boite 105, 4 place Jussieu, F-75252 Paris CEDEX 5, France. (faycal.rejiba@upmc.fr; cyril.schamper@upmc.fr)

F. Sagnard, Laboratoire Central des Ponts et Chaussées, MACS, 58 blvd. Lefebvre, F-75732 Paris CEDEX 15, France. (sagnard@lcpc.fr)